CHEMISTRY
A EUROPEAN JOURNAL

DOI: 10.1002/chem.200700175

Preparation and Characterization of a Novel Organic–Inorganic Nanohybrid "Cerasome" Formed with a Liposomal Membrane and Silicate Surface

Kiyofumi Katagiri,*[a, b] Mineo Hashizume,[a] Katsuhiko Ariga,[a, c] Takashi Terashima,[a] and Jun-ichi Kikuchi*[a]

Abstract: A novel class of organic–inorganic hybrids, the so-called cerasomes, which have a bilayer vesicular structure and a silicate surface, has been synthesized by combination of sol–gel reaction and self-assembly of organoalkoxysilanes with a molecular structure analogous to lipids. We have synthesized two cerasome-forming organoalkoxysilanes, *N*-[*N*-(3-triethoxysilyl)propylsuccinamoyl]dihexadecylamine (**1**) and *N*,*N*-dihexadecyl-*N*$^{\alpha}$-[6-[(3-triethoxysilyl)propyldimethylammonio]hexanoyl]glycinamide bromide (**2**), and investigated the synthetic conditions of the cerasomes and their structural characteristics. For the proamphiphilic **1**, the cerasome was obtained under restricted pH conditions where acid-catalyzed hydrolysis of the triethoxysilyl moiety proceeded without disturbing the vesicle formation. In contrast, the amphiphilic **2**, additionally having a hydrophilic quaternary ammonium group, formed stable dispersions of the cerasome in a wide pH range. The hydrolysis behavior of the triethoxysilyl groups was monitored by ^{1}H NMR spectroscopy. Morphology of the cerasomes having the liposomal vesicular structure was confirmed by TEM observations. Extent of the development of siloxane networks through condensation among the silanol groups on the cerasome surface was evaluated by using MALDI-TOF-MS spectrometry. Formation of oligomers of the cerasome-forming lipids in the vesicle was clearly confirmed. Due to the siloxane network formation, the cerasome showed remarkably high morphological stability compared with a reference liposome, as evaluated by surfactant dissolution measurements.

Keywords: lipid bilayers · organic–inorganic hybrid composites · self-assembly · sol–gel processes

Introduction

Organic–inorganic hybrid materials have attracted much attention from material scientists and chemists in recent years, due to their great potential for use in a wide variety of applications through fusion of individual organic and inorganic properties.[1–4] Up to the present time, various kinds of material combinations and synthetic strategies have been developed. The sol–gel method is one of the most powerful techniques to prepare hybrid materials and has provided moderate preparative conditions for construction of inorganic oxide frameworks that are derived from hybrid materials.[5] Especially preparation of novel materials with organized nanostructures is a fascinating research subject in the field of hybrid materials.[6–12] These approaches are generally based on the sol–gel technique in the presence of molecular assemblies as the templates, such as rod-like micelles,[13–15] block-copolymers,[16–18] microemulsions,[19,20] organogels,[21] cast films of bilayer membranes[22] and bilayer vesicles.[23] Thus the properties of nanohybrids depend on their nanostructures, especially the structure at the interface between the inorganic and organic components. Pre-organization employing electrostatic and hydrogen-bonding interactions between an organic template and an inorganic precursor is realized to be very important. However, the interface between

[a] Dr. K. Katagiri, Dr. M. Hashizume, Dr. K. Ariga, T. Terashima, Prof. J.-i. Kikuchi
Graduate School of Materials Science
Nara Institute of Science and Technology (NAIST)
8916-5 Takayama, Ikoma, Nara 630-0192 (Japan)
E-mail: katagiri@apchem.nagoya-u.ac.jp
jkikuchi@ms.naist.jp

[b] Dr. K. Katagiri
Present address:
Graduate School of Engineering
Nagoya University, Furo-cho, Chikusa-ku
Nagoya 464-8603 (Japan)
Fax: (+81) 52-789-3201

[c] Dr. K. Ariga
Present address
Supermolecules Group
National Institute for Materials Science (NIMS)
1-1 Namiki, Tsukuba, Ibaraki 305-0044 (Japan)

the organic and inorganic components in these hybrids seems to be structurally ambiguous, and difficult to control at the molecular level compared with the individual component structures. In addition, most of these materials are finally composed of inorganic components alone and the organic parts are simply employed as templates. In contrast, a novel class of layered organic–inorganic nanocomposites, composed of amphiphilic molecules with a covalent bond between the silicate and the surfactant, have been developed in recent years.[24–28] These materials would offer much potential, since the hybrid precursors can form three-dimensional networks during the self-assembling process whereby inorganic layers and organic moieties are covalently linked with stable Si–C bonds.

We have recently developed a novel type of the organic–inorganic nanohybrids "cerasome" in aqueous media through a combination of sol–gel reaction and self-assembling of lipidic organotrialkoxysilanes to form bilayer vesicles covered with a silicate surface.[29a] We have first prepared a proamphiphilic organoalkoxysilane (**1**) with a triethoxysilyl head moiety, a hydrophobic double-chain segment and a connector unit between them. Upon applying the sol–gel technique to compound **1**, the resulting amphiphiles with a silanol head aggregated to form morphologically stable bilayer vesicles. The cerasome is composed of a spherical lipid-bilayer membrane having an internal aqueous compartment, like a so-called liposome,[30–35] and additionally covered with a silicate framework on its surface (Figure 1). We have also designed another cerasome-forming lipid (**2**) having a quaternary ammonium group at the head moiety in addition to the triethoxysilyl part. While liposomes are widely used as not only for biomembrane models but also for functional nanocapsules, their morphological instability is always one of the serious problems for practical applications. The cerasome was expected to overcome this problem by the existence of a silicate layer on its surface. In addition, we can say that the cerasome is a novel organic–inorganic nanohybrid having precisely designed nanostructure. That is, the thickness of both organic and inorganic layer of the cerasome is attributed to the molecular structure of the cerasome-forming lipid, and the vesicular size of the cerasome is basically controllable, by applying conventional methodologies for preparing monodispersed liposomes.

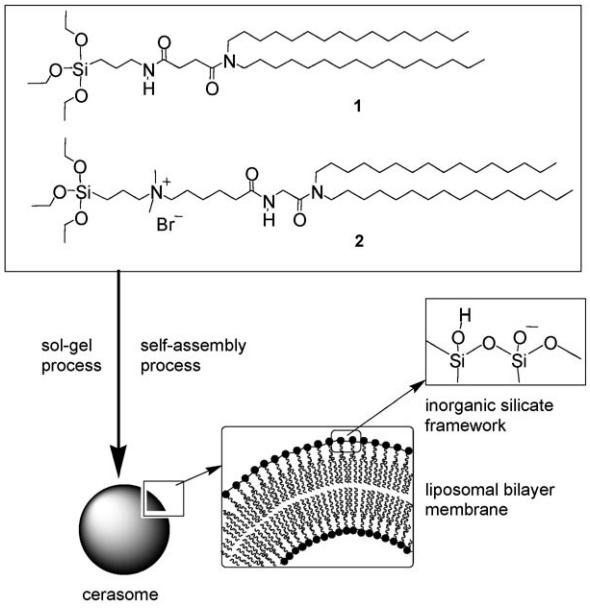

Figure 1. Molecular structures of the cerasome-forming lipids (**1** and **2**) and schematic drawing of the cerasome.

In this article, we report in detail the preparation and characterization of cerasomes derived from the lipidic organoalkoxysilanes **1** and **2**. We investigated in participation of the head group of the lipid molecules during the hydrolysis in the cerasome formation, especially focusing on the correlations between the sol–gel process and pH conditions. In addition, characterization of the cerasomes was performed by various physical measurements in order to clarify the relationships between the molecular structure of the cerasome-forming lipids and the resulting morphology and physicochemical properties.

Results and Discussion

Molecular design of the cerasome-forming lipid: The basic idea for designing a bilayer-forming lipid can be referred to the concept of the critical packing parameters for lipid assemblies.[36] In addition, we considered the importance of the connector part,[37] which can form intermolecular hydrogen bonding to add morphological stability to the lipid assembly, between the hydrophobic alkyl chains and the hydrophilic part in the lipid molecule. We previously revealed the effect of the connector part by systematic investigations of so-called peptide lipids, which have amino acid or oligopeptide moieties between the hydrophobic and the hydrophilic part.[34] Our first design of the cerasome-forming lipid took into account these points, and also the simplicity of synthesis. In addition, the silanol group was capped by ethoxy groups because of its instability under air. Lipidic organoalkoxysilane **1** can be synthesized by simple condensation reactions between the three molecular units, dihexadecyamine, succinic anhydride, and 3-aminopropyltriethoxylsilane. After hydrolyzing the triethoxysiliyl group, **1** is expected to become suitable structure to form lipid bilayer. Another lipid, that is, lipid **2** used the same framework of the typical peptide lipid,[34] in which the dihexadecylamine unit and quaternary ammonium group sandwiched glycine unit and pentamethylene chain, and one of the methyl group of the trimethylammonium group was replaced by 3-triethoxypropyl group. Contrary to lipid **1**, lipid **2** can act as an amphiphilic molecule even if its silanol group is capped by ethoxy groups. Lipid **2** was expected to show similar physical parameters such as phase-transition temperature as those of the corresponding peptide lipid.

pH Dependence for hydrolysis of the triethoxysilyl moiety: As for the lipidic organoalkoxysilane **1**, hydrolysis of the triethoxysilyl head group converts the proamphiphile into the corresponding amphiphilic lipid to form a self-assembly of the liposome-like bilayer membrane. In addition, condensation among the silanol groups on the relatively hydrophobic vesicular surface would proceed to develop a silica-like inorganic framework, or a siloxane network. However, if the hydrolysis and subsequent condensation occur much quicker prior to the self-assembling, formation of the bilayer structure may be disturbed. Therefore, control of the reaction rate in the sol–gel process, especially the hydrolysis rate, seems to be important for the cerasome formation.

At first, we investigated the monolayer property of lipid **1** and **2** on water at various pH conditions by measurements of the surface pressure (π)–molecular area (A) isotherms (Figure 2a). In the case of lipid **1**, the π–A isotherm on pure

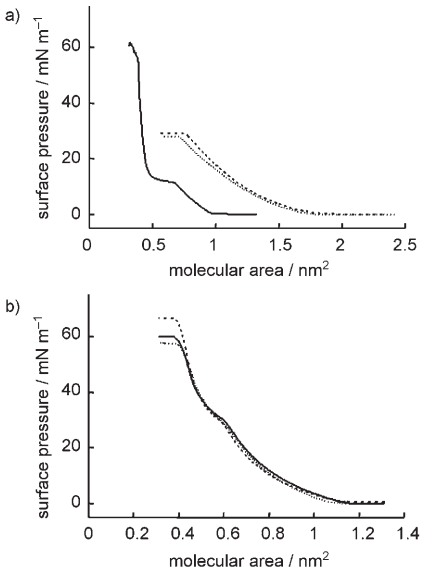

Figure 2. π–A Isotherms of a) **1** and b) **2** on aqueous H_2SO_4 (pH 2, ——), pure water (pH 6, -----) and aqueous NH_4OH (pH 12, •••••) at 20 °C.

water at pH 6 gave a presence of an expanded phase and collapsed at low pressure (27 mN m^{-1}) before reaching a less compressible region, similar to observations at pH 12. On the other hand, in the case of the π–A isotherm at pH 2, transition from an expanded phase to a condensed phase was clearly observed and the collapsed pressure was found to be much higher. The limiting area evaluated from the latter isotherm was 0.46 nm^2, indicating a well-packed state of the dialkyl chains. These results imply that the acid-catalyzed hydrolysis of the proamphiphilic compound **1** and followed condensation proceeds to give a well-packed amphiphilic monolayer around pH 2. Therefore, the acid catalysis seems to be suitable for the conversion of compound **1** to the corresponding amphiphilic form being capable of self-assembly. Our previous results for the dispersion states of lipid **1** after vortex mixing in aqueous media show that lipid **1** does not molecularly change to an amphiphilic form and remains as oil droplets at neutral pH. It is probably due to the extremely slow hydrolysis of the head group. On the other hand, a translucent solution characteristic of a liposomal dispersion is obtained under moderate acidic conditions at pH 3 where hydrolysis of the ethoxysilyl groups is gently preceded by acid catalysis. Under stronger acidic conditions (pH 1), however, a stable dispersion is not obtained and precipitation is observed immediately. In this case, the hydrolysis and subsequent condensation reaction were so fast that a vesicular structure could not be formed. At pH 12, the resulting solution was translucent but oil droplets still remained. Thus, the hydrolysis seemed to proceed heterogeneously under the basic conditions.

The different behavior observed under the present pH conditions can be explained on the basis of the generally accepted mechanism for hydrolysis of alkoxysilane compounds in the sol–gel process.[5] Under acidic conditions, hydrolysis of the triethoxysilyl group proceeds equally for each of the molecules in a one-by-one manner. This process would provide a suitable condition for the preparation of the bilayer assembly from lipid **1**. On the other hand, under basic conditions, particular molecules are preferentially hydrolyzed while the other molecules remain as unreacted species. This process leads to heterogeneous hydrolysis and various reaction stages of lipid **1** are observed. Thus, basic conditions seem to be unsuitable for the preparation of cerasomes.

In the case of the π–A isotherms for lipid **2** (Figure 2b), transition from an expanded phase to a condensed phase was clearly observed and the collapsed pressure was sufficiently high under all pH conditions examined. These results are different from those of lipid **1**, presumably reflecting that lipid **2** bearing a quaternary ammonium group is capable of forming monolayer membrane regardless of the hydrolysis states of the triethoxysilyl moiety. As for the cerasome derived from **2**, homogeneous aqueous dispersions were obtained under all pH conditions examined. The resulting dispersions were so stable that the turbidity did not change over 12 h. Thus monolayer properties of the cerasome-forming lipids at the air–water interface are useful to evaluate appropriate preparation conditions for the cerasome formation in aqueous media.

The hydrolysis behavior of lipids **1** and **2** was monitored by ^{1}H NMR spectroscopy. ^{1}H NMR spectra of the aqueous dispersion of **1** at pD 7 showed a broad quartet signal at δ 3.75 ppm corresponding to the methylene protons in the ethoxy group of the lipid ($(CH_3CH_2O)_3Si$-). No signal assigned to hydrolyzed product was detected even after a 12 h incubation period at 25 °C. On the other hand, at pD 3 the broad signal for the methylene protons in the ethoxy group of the lipid gradually decreased to be replaced by a sharp quartet signal at δ 3.65 ppm, which is assigned to the methylene protons of ethanol as a product of the hydrolysis reaction. Time course for the hydrolysis of **1**, as evaluated from the peak area changes in the methylene proton signal of the produced ethanol, are shown in Figure 2. While the hydrolysis hardly proceeded at pD 7 (Figure 3a), slow hydrolysis

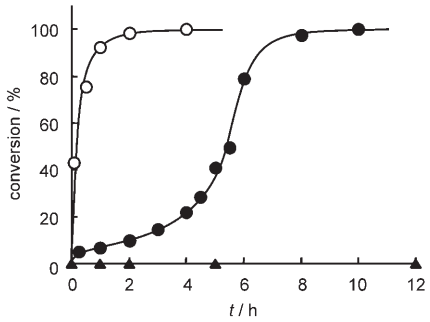

Figure 3. Time courses for the cerasome formation process as evaluated from the hydrolysis of the lipids (1.0 mmol dm^{-3}) in D_2O at pD 3 and 25 °C. **1** at pD 7 (▲); **1** at pD 3 (●); **2** at pD 3 (○).

was observed at pD 3 in the initial stage of the reaction followed by a gradual rate acceleration showing a sigmoidal curve to complete after 8 h (Figure 3b). Such behavior is due to a change in the reaction system from a heterogeneous to a homogeneous state with time, since lipid **1** is less soluble in water and is initially present as oil droplets. On the other hand, hydrolysis of lipid **2** proceeded rapidly to complete within 2 h under the similar pD conditions (Figure 3c). The results imply that amphiphilic lipid **2** spontaneously forms bilayer vesicles prior to hydrolysis and that the hydrolysis of the triethoxysilyl head efficiently occurs on the vesicular surface.

Morphology of the cerasome: The aggregate structures of the cerasomes were observed by transmission electron microscopy (TEM). The cerasomes were prepared in aqueous HCl at pH 3.0 at a lipid concentration of 0.5 mmol dm^{-3}. Formation of the multilamellar vesicles (MLVs) with a lipid bilayer thickness of about 4 nm and a vesicular diameter of 200 nm in the slightly turbid aqueous dispersion of **1** under vortex mixing was clearly confirmed by the TEM images, similar as our previous report.[29a] Ultrasonication of the aqueous dispersion with a probe-type sonicator for 20 min at 30 W gave a clear solution with low-surface tension. The electron micrographs showed the presence of cerasomes with a diameter range from 150 to 300 nm, which sizes correspond to the hydrodynamic diameter (214 nm) as evaluated by dynamic light scattering (DLS) measurements. Unlike conventional liposomes, ultrasonication did not alter the structure of the cerasome **1** from MLVs to single unilamellar vesicles (SUVs).

The TEM images of the cerasome prepared from lipid **2** are shown in Figure 4. Cerasome **2** is directly prepared in the presence of a staining agent. The vesicles in a diameter range from 50 to 100 nm were observed for cerasome **2** prepared by vortex mixing (Figure 4a). An internal view of the MLVs with a bilayer thickness of about 5 nm was clearly confirmed. Upon sonication of the dispersion sample with a probe-type sonicator for 10 min at 30 W, smaller particles with a diameter of 20–40 nm were observed (Figure 4b), which suggests formation of SUVs of the cerasome. The vesicular size was well consistent with the hydrodynamic diameter (30 nm) as evaluated by DLS measurements.

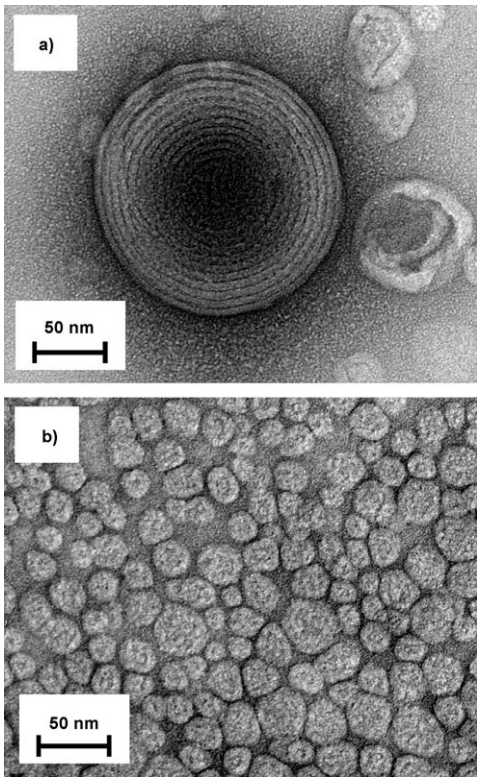

Figure 4. TEM images of the cerasome of **2** prepared by a) vortex mixing and followed by b) ultrasonication. The cerasome dispersions were prepared in the presence of the negative staining agent.

The formation of siloxane bonds on the cerasome surface was examined by FT-IR spectroscopy. Stretching bands assigned to the Si-O-Si and Si-OH groups were observed around $\tilde{\nu}$ 1100 and 950 cm^{-1}, respectively.[38] The former peak intensity was much weaker than the latter in cerasomes both derived from **1** and **2** in the aqueous dispersion state. Thus it is suggested that the cerasomes have a silica-like surface with siloxane frameworks but the degree of polymerization is not so high. The detectable species of the lipid oligomers in cerasome **1** as evaluated by MALDI-TOF-MS spectra were listed in Table 1. Trimethylsilylation was performed for the aqueous dispersion samples of the cerasome prepared after 15 min and 10 h. While the monomer, dimer and trimer species were detected in the sample prepared after 15 min, oligomers with higher molecular weight such as tetramers and pentamers were additionally detected for the sample during prolonged incubation. It seems that the siloxane network grew with increasing incubation time. From cryoscopic measurements, the number-average molecular weight, M_n, was determined to be 1300 for the aqueous dispersion of the cerasome **1** incubated for 10 h. This value corresponds to the molecular weight of the dimer species. On the other hand, the size of the cerasomes did not practically change after enough incubation time as confirmed by TEM and DLS measurements. Accordingly, the siloxane

Table 1. Detectable species of lipid oligomers for the cerasome of **1** as evaluated by MALDI-TOF-MS spectra.

Oligomer species	Calcd	Detected molecular weight[a]	
	M_w	Incubation for 15 min	Incubation for 10 h
monomer	900.7	901.7	901.7
dimer	1641.0	1640.4	1640.4
trimer (cyclic)	2217.9	ud	ud
trimer (linear)	2380.3	2380.3	2380.3
tetramer (cyclic or branched)	2957.3	ud	2957.3
tetramer (linear)	3119.6	ud	3117.4
pentamer (cyclic or branched)	3696.7	ud	3695.3
pentamer (linear)	3859.0	ud	ud

[a] ud: undetectable.

network is not so highly developed on the cerasome surface. These observations are also supported by the computer-aided molecular model study since the length of the Si-O-Si bond is much shorter than the diameter of the cross-section of the dialkyl tail.

Surfactant dissolution of the cerasomes: Surfactant solubilisation is a useful method to evaluate morphological stability of liposomes in aqueous media.[35c,39] For example, Regen et al. reported that polymerized liposomes were morphologically highly stable against unpolymerised liposomes towards lysing agents such as ethanol and surfactants.[35a,c] Figure 5

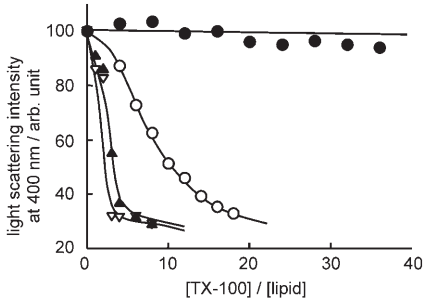

Figure 5. Light scattering intensities of the cerasomes prepared from **1** or **2**, and DMPC-liposome as a function of added equivalents of TX-100 at 25 °C: cerasome of **1** incubated for 24 h (●); cerasome as-prepared from **1** (○); cerasome of **2** incubated for 24 h (▲); DMPC-liposome (▽).

shows the resistance of cerasomes against a nonionic surfactant TX-100 as determined by the light scattering intensity of the vesicles. Liposomal membrane formed with dimyristoylphosphatidylcholine (DMPC) was used as a reference. When three equivalents of TX-100 were added to the DMPC liposome, the light scattering intensity was drastically decreased indicating a collapse of the vesicle. In contrast to the DMPC liposome, the cerasome prepared from lipid **1** exhibited remarkable morphological resistance toward TX-100. The light scattering intensity of the cerasome incubated for 24 h did not changed at all even in the presence of 36 equivalents of TX-100. Such surprising morphological stability of cerasome **1** was also confirmed by the DLS measurements. Morphological stability of the present cerasome seems to be superior to that of an excellent example of the polymerized liposomes recently developed by O'Brien et al.[39] It is noteworthy that the resistance of cerasome **1** toward TX-100 was not sufficient immediately after preparation. Judging from the results in Table 1 and Figure 5, it is clear that morphological stability of the cerasome comes from development of the siloxane network on the vesicular surface. As for cerasomes prepared from lipid **2**, the resistance against TX-100 is comparable to that of the conventional liposome even after prolonged incubation. It seems that the quaternary ammonium group of lipid **2** strongly interacts with oligo(ethyleneglycol) group of TX-100 to destabilize the vesicular structure. It is supported by the fact we found quite recently that cerasome **2** has a high morphological stability against other kinds of surfactants, such as cetyltrimethylammonium bromide (CTAB), which completely dissolved DMPC liposomes.[40] Accordingly, we can control the morphological stability of the bilayer vesicles through modification of molecular design of the cerasome-forming lipids.

Phase-transition behavior of the cerasomes: Phase-transition parameters (enthalpy change from gel to liquid-crystalline state, ΔH, and temperature at the peak maximum, T_m) for the cerasomes were measured by DSC. The concentration of the cerasome-forming lipid for the DSC measurements was fixed to 2.0 mmol dm^{-3}. ΔH and T_m for the aqueous dispersion of the cerasome prepared from lipid **1** were 47.5 kJ mol^{-1} and 10.5 °C, respectively. Upon ultrasonication of cerasomes with a probe-type sonicator for 10 min at 30 W, the ΔH value decreased to 11.5 kJ mol^{-1} whereas the T_m value did not change. For cerasome **2** in the aqueous dispersion state, the ΔH and T_m values were 33.3 kJ mol^{-1} and 25.7 °C, respectively. These phase-transition parameters were comparable to those for peptide lipids previously reported.[34] Upon ultrasonication of cerasome **2** with a probe-type sonicator for 10 min at 30 W, the endothermic peak for phase transition apparently disappeared. We have previously clarified that the transformation of MLV to the corresponding single unilamellar vesicle is reflected in the decrease of both the ΔH and T_m values.[34] In addition, ΔH is more sensitive than T_m to such morphological changes. Since it is well known that MLVs formed with the conventional liposomes generally transform to SUVs under the ultrasonication conditions employed in this study, cerasome **1** is more tolerant towards morphological changes than the liposome-forming lipids. Formation of the siloxane network on the vesicular surface would prevent such morphological transformations.

Zeta-potential of the cerasomes: The pH dependences of surface charges of cerasomes **1** and **2** were evaluated by zeta-potential measurements (Figure 6). The cerasomes were prepared in aqueous NaCl (10 mmol dm^{-3}) at pH 3.0 with a lipid concentration of 1.0 mmol dm^{-3} and followed

ultrasonication with a probe-type sonicator for 10 min at 30 W. The zeta-potential of cerasome **1** changed from +10 to −70 mV depending on the medium pH (Figure 6a). The isoelectric point (IEP) of the cerasomes was found to be 4.3. Cerasome **1** had large negative charges under neutral and basic conditions, reflecting deprotonation of the silanol groups on the cerasome surface. It is well known that the IEP values for the typical silica particles derived from the sol–gel method lie in the region of 2–3 and have a zeta-potential ranging from +20 to −80 mV in the analogous pH region.[41,42] The results imply that the surface electrical state of cerasome **1** resembles that of the silica particles. In addition, the IEP value for the cerasome was somewhat larger than those for the silica particles, presumably due to the electron-donating character of the alkyl group bound to the silicon atom in the former. On the other hand, the IEP value shifted to 12.0 for the cerasome prepared from lipid **2** (Figure 6b). In a pH range lower than 12.0, the zeta-potential of the cerasome increased with a decrease in pH to reach +70 mV at pH 6. This value was considerably higher than the maximal zeta-potential of cerasome **1**. Such difference is attributable to the existence of a quaternary ammonium group in lipid **2**. At neutral pH, cerasome **1** acts as a polyanionic vesicular particle, whereas cerasome **2** is polycationic. Thus we can control the IEP value of the cerasome to a desired value between 4 and 12 by mixing lipids **1** and **2** in an appropriate ratio.

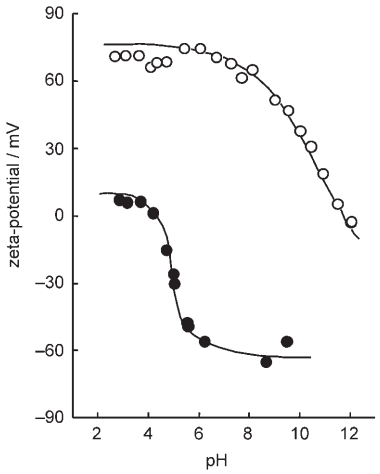

Figure 6. pH Dependence of zeta-potential for the cerasomes: cerasome of **1** (●); cerasome of **2** (○).

The hydrodynamic diameters for the cerasome **1** at various pH values were evaluated by DLS measurements (Figure 7). The cerasome was prepared in aqueous HCl at pH 3.0 with a lipid concentration of 1.0 mmol dm^{-3} and followed ultrasonication with a probe-type sonicator for 10 min at 30 W. The hydrodynamic diameter and polydispersity index of the cerasome at pH 3 was 214 nm and 0.155, respectively. The hydrodynamic diameter did not change in the regions below pH 4 and above pH 6. In a pH region around the IEP value, however, the hydrodynamic diameter was increased drastically to form the low dispersive vesicular aggregates due to the loss of charges on the cerasome surface.

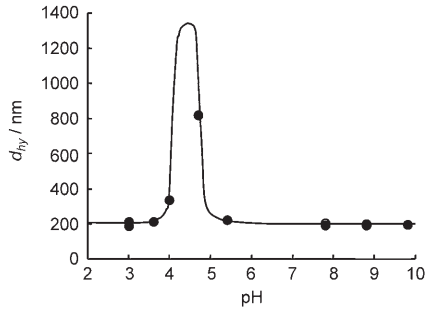

Figure 7. pH Dependence of hydrodynamic diameter for the cerasomes of **1** prepared upon sonication of the aqueous dispersion at pH 3. The measurements were done immediately after pH adjustment.

Conclusion

In this article, we have demonstrated that novel organic–inorganic hybrid materials, the so-called cerasomes, which consist of a liposomal bilayer structure and a silicate framework on their surfaces, and can be prepared by applying the sol–gel method for two lipidic organoalkoxysilanes. Characteristic vesicle parameters for the cerasomes are listed in Table 2. The cerasome formation is dependent on the molecular structure of the organoalkoxysilanes, in particular on the head group of the lipids. For a proamphiphilic **1** the preparation of the cerasome was limited to moderate acidic conditions. In contrast, the cerasome was readily prepared over a wide pH range for amphiphilic **2** having a quaternary ammonium moiety, since the hydrolysis and self-assembling processes proceeded independently. The results indicate that structural differences in the head moiety of the lipids have a significant influence on the cerasome-formation process, particularly with regards to the hydrolysis step. The vesicular form of the cerasome was observed by TEM images. The cerasomes prepared by vortex mixing of the aqueous disper-

Table 2. Characteristic vesicle parameters for the cerasomes prepared from the lipids **1** and **2**

Parameter entity	Cerasome of **1**	Cerasome of **2**
available pH region for preparation	around 3	2–12
reaction time for hydrolysis at pH 3 h	10	2
phase transition temperature[a]/°C	10.5	25.7
phase transition enthalpy change[a]/kJ mol^{-1}	47.5	33.3
hydrodynamic diameter[b]/nm	214	30
isoelectric point[b]	4.3	12.0

[a] Aqueous dispersion state. [b] Ultrasonicated sample with a probe-type sonicator for 10 min at 30 W.

sion have a multi-walled bilayer structure and, as for cerasome **2**, can be further transformed into a single-walled vesicle upon ultrasonication. Formation of the lipid oligomers in the cerasome was confirmed by FT-IR spectroscopy and MALDI-TOF-MS spectrometry. Morphological stability of the cerasome is much superior than that of conventional liposomes; this mainly results from the siloxane network formed on the vesicular surface. DSC measurements revealed that the cerasomes possess phase transitional behavior from gel to liquid-crystalline states, in analogous to the liposomes. This means that the cerasome is a unique nanohybrid which has both highly stable entire structure and mobile inside nanostructure. In addition, the zeta-potential and isoelectric point of the cerasome can be controlled easily by changing the molecular design of the lipids. We believe that the cerasome can open a new field in constructing organic–inorganic nanohybrid materials. On the basis of these findings, optimization of molecular design for a super-stable cerasome with a well-developed silicate surface and its functionalisation are in progress in our laboratory.

Experimental Section

Materials: Unless otherwise stated all reagents and chemicals were obtained commercially and used without further purification. Succinic anhydride, *N*,*N*′-dicyclohexylcabodiimide (DCC) and 50% dimethylamine solution were obtained from Wako Pure Chemical Industries, Ltd. 3-Aminopropyltriethoxysilane, 3-bromopropyltriethoxysilane and trimethylchlorosilane were purchased from Shin-Etsu Chemical Co., Ltd. *N*-(*tert*-Butoxycarbonyl)glycine and 6-bromohexanoyl chloride were obtained from Peptide Institute, Inc., and Aldrich Chemical Company, Inc., respectively. Dihexadecylamine were prepared by reaction of hexadecylamine with 1-bromohexadecane in the presence of sodium carbonate and purified by recrystallisation from ethanol. For the cerasome preparation, distilled and deionised water was used and prepared using an Autostill WS33 (Yamato Scientific) and Milli-Q Labo (Nihon Millipore), respectively.

Dry solvents for syntheses were purified as follows: Dichloromethane was distilled on calcium hydride. Tetrahydrofuran (THF) was distilled after refluxing with sodium and benzophenone. *N*,*N*-Dimethylformamide (DMF) was distilled at 50–60 °C under a reduced pressure of 20–30 mmHg after drying overnight with DRIERITE. ^{1}H and ^{13}C NMR Spectra were recorded on a JEOL JNM-LA400 or JNM-EX270 spectrometer in $CDCl_3$ with tetramethylsilane (TMS) as an internal reference. Melting points were recorded on a Yanaco MP-500D melting point apparatus (hot-plate type) with a filter for polarized light. Column chromatography was performed using silica gel (Wako gel C-300, Wako Pure Chemical Industries, Ltd.); thin-layer chromatography on Wako silica gel 70FM plates.

Synthesis of the cerasome-forming organotriethoxysilanes: Synthetic routes for lipids **1** and **2** are shown in Schemes 1 and 2, respectively. The route for **1** was referred to that for the lipid having analogous framework.[43]

***N*,*N*-Dihexadecylsuccinamic acid (3)**: Dihexadecylamine (3.00 g, 6.44 mmol) and succinic anhydride (1.29 g, 12.9 mmol) were added to dry THF (50 mL) and dissolved upon heating. The solution was stirred for 24 h at room temperature. The solvent was evaporated in vacuo and the crude product was dissolved in dichloromethane (50 mL). The solution was then washed with 10% aqueous citric acid and saturated aqueous

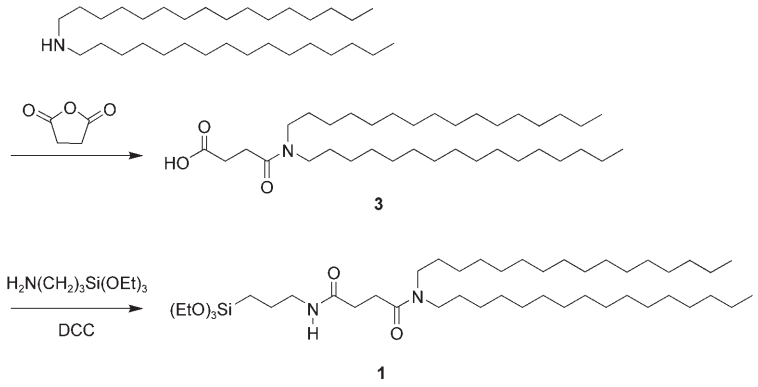

Scheme 1.

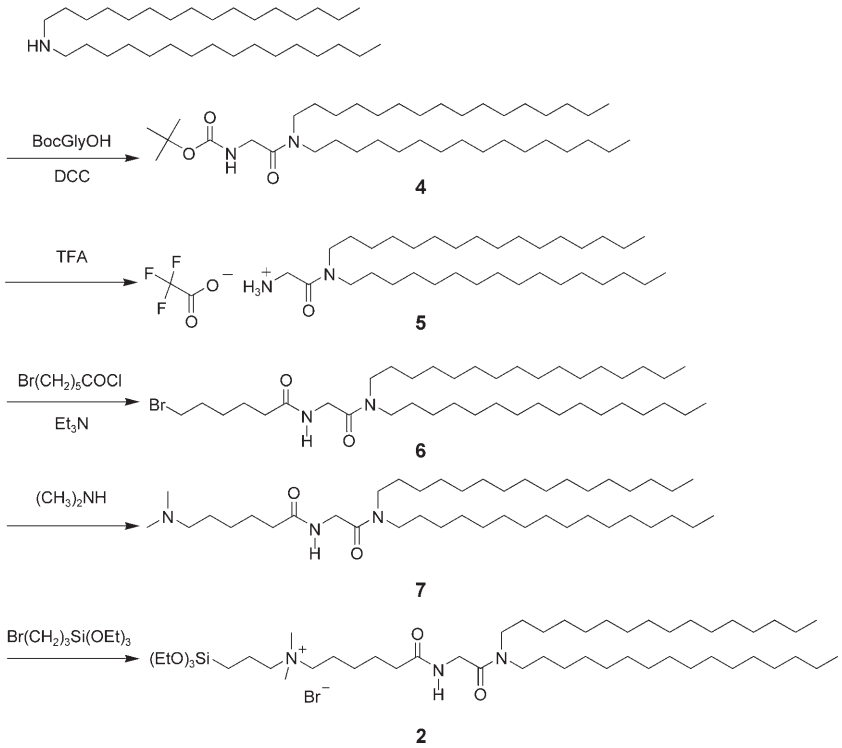

Scheme 2.

sodium chloride in this sequence. After removing residual water using phase separation filter paper, the solvent was evaporated in vacuo. Subsequent recrystallization from acetonitrile gave a white solid (2.87 g, 78.8%). M.p. 58.1–58.4°C; TLC: R_f=0.50 (hexane/ethyl acetate/acetic acid 90:30:1); ^{1}H NMR (400 MHz, $CDCl_3$, 25°C, TMS): δ=0.88 (t, J=6.6 Hz, 6H, $NCH_2CH_2(CH_2)_{13}CH_3$), 1.26 (m, 52H, $NCH_2CH_2(CH_2)_{13}CH_3$), 1.54 (m, 4H, $NCH_2CH_2(CH_2)_{13}CH_3$), 2.69 (m, 4H, $HOCO(CH_2)_2CON$), 3.15 (t, 2H, J=7.8 Hz, $NCH_2CH_2(CH_2)_{13}CH_3$), 3.32 ppm (t, 2H, J=7.8 Hz, $NCH_2CH_2(CH_2)_{13}CH_3$).

***N*-[*N*-(3-Triethoxysilyl)propylsuccinamoyl]dihexadecylamine (1)**: DCC (1.01 g, 4.90 mmol) was added with stirring at 0°C to a solution of **3** (2.40 g, 4.24 mmol) in dry dichloromethane (50 mL). After 15 min of stirring, 3-aminopropyltriethoxysilane (1.22 g, 5.51 mmol) was added to the solution and the mixture was stirred for 4 h at 0°C and subsequently for a further 12 h at room temperature. Precipitates (*N*,*N*′-dicyclohexylurea) were removed by filtration. The solvent was evaporated in vacuo and residual oil was dissolved in ethyl acetate (50 mL). The solution was cooled overnight at 4°C and the further precipitated *N*,*N*′-dicyclohexylurea was removed by filtration. The mixture was evaporated in vacuo and the crude product was purified by column chromatography. Impurities were eluted with ethyl acetate/chloroform 1:9; subsequent elution with 100% ethyl acetate gave a colorless oil (1.70 g, 52.1%). TLC: R_f=0.28 (chloroform/ethyl acetate 20:1); ^{1}H NMR (400 MHz, $CDCl_3$, 25°C, TMS): δ=0.62 (t, J=8.4 Hz, 2H, $SiCH_2$), 0.88 (t, J=6.6 Hz, 6H, $NCH_2CH_2(CH_2)_{13}CH_3$), 1.22 (t, J=7.3 Hz, 9H, $SiOCH_2CH_3$), 1.22–1.29 (m, 52H, $NCH_2CH_2(CH_2)_{13}CH_3$), 1.60 (br, 6H, $NCH_2CH_2(CH_2)_{13}CH_3$, $SiCH_2CH_2CH_2NH$), 2.51 (t, J=6.6 Hz, 2H, $NCOCH_2$), 2.64 (t, J=6.6 Hz, 2H, $NCOCH_2$), 3.15–3.24 (m, 6H, $NCH_2CH_2(CH_2)_{13}CH_3$, $SiCH_2CH_2CH_2NH$), 3.80 (q, J=7.3 Hz, 6H, $SiOCH_2CH_3$), 6.30 ppm (br, 1H, NHCO); ^{13}C NMR (100 MHz, $CDCl_3$, 25°C, TMS): δ = 172.58, 171.39, 58.45, 48.03, 46.33, 42.00, 31.97, 31.89, 29.75, 29.71, 29.68, 29.62, 29.49, 29.41, 28.99, 27.85, 27.15, 27.01, 22.96, 22.73, 18.32, 14.14, 7.76 ppm; HRMS (FAB$^+$): m/z: calcd for $C_{45}H_{93}N_2O_5Si$: 769.6854; found: 769.6857 $[M+H]^+$; elemental analysis calcd (%) for $C_{45}H_{92}N_2O_5Si$: C 70.31, H 12.05, N 3.65; found: C 70.26, H 12.05, N 3.64.

***N*,*N*-Dihexadecyl-*N*$^\alpha$-(*tert*-butoxycarbonyl)glycinamide (4)**: DCC (5.98 g, 29.0 mmol) was added with stirring at 0°C to a solution of *N*-(*tert*-butoxycarbonyl)glycine (4.40 g, 25.2 mmol) in dry dichloromethane (160 mL). After 15 min, *N*,*N*-dihexadecylamine (11.7 g, 25.2 mmol) was added to the solution and the mixture was stirred for 4 h at 0°C and for a further 12 h at room temperature. Precipitates (*N*,*N*′-dicyclohexylurea) were removed by filtration. The solvent was evaporated in vacuo and the residual oil was dissolved in ethyl acetate (160 mL). The solution was cooled overnight at 4°C and the further precipitated *N*,*N*′-dicyclohexylurea was removed by filtration. The solution was then washed with 10% aqueous citric acid, saturated aqueous sodium chloride, 4% aqueous sodium hydrogen carbonate and saturated aqueous sodium chloride in this sequence. After removing residual water by using phase separation filter paper, the solvent was evaporated in vacuo. The residue was purified on a column of silica gel with ethyl acetate/chloroform 1:9 to give a colorless oil (9.70 g, 61.8%). TLC: R_f=0.60 (hexane/ethyl acetate 3:1); ^{1}H NMR (400 MHz, $CDCl_3$, 25°C, TMS): δ = 0.88 (t, J=6.8 Hz, 6H, $NCH_2CH_2(CH_2)_{13}CH_3$), 1.24–1.29 (m, 52H, $NCH_2CH_2(CH_2)_{13}CH_3$), 1.45 (s, 9H, $(CH_3)_3CO$), 1.53 (m, 4H, $NCH_2CH_2(CH_2)_{13}CH_3$), 3.15 (t, J=7.8 Hz, 2H, $NCH_2CH_2(CH_2)_{13}CH_3$), 3.30 (t, J=7.8 Hz, 2H, $NCH_2CH_2(CH_2)_{13}CH_3$), 3.94 (d, J=5.9 Hz, 2H, $NHCH_2CO$), 5.56 ppm (br, 1H, $(CH_3)_3CONH$).

***N*,*N*-Dihexadecylglycinamide trifluoroacetic acid salt (5)**: Trifluoroacetic acid (10.0 g, 87.7 mmol) was added to **4** (6.50 g, 10.4 mmol) and the mixture was stirred for 4 h at room temperature. Evaporation of an excess amount of trifluoroacetic acid in vacuo below 40°C gave colorless oil. The crude product was purified by recrystallization from acetonitrile to give a white powder (6.01 g, 90.8%). M.p. 50.2–50.7°C; ^{1}H NMR (400 MHz, $CDCl_3$, 25°C, TMS): δ=0.88 (t, J=6.8 Hz, 6H, $NCH_2CH_2(CH_2)_{13}CH_3$), 1.24–1.29 (m, 52H, $NCH_2CH_2(CH_2)_{13}CH_3$), 1.53 (m, 4H, $NCH_2CH_2(CH_2)_{13}CH_3$), 3.15 (t, J=7.8 Hz, 2H, $NCH_2CH_2(CH_2)_{13}CH_3$), 3.30 (t, J=7.8 Hz, 2H, $NCH_2CH_2(CH_2)_{13}CH_3$), 3.94 ppm (d, J=5.9 Hz, 2H, $NHCH_2CO$).

***N*,*N*-Dihexadecyl-*N*$^\alpha$-(6-bromohexanoyl)glycinamide (6)**: Triethylamine (2.86 g, 28.3 mmol) and **5** (3.00 g, 4.71 mmol) were dissolved in dry dichloromethane (30 mL) and the solution was cooled to 0°C. 6-Bromohexanoyl chloride (2.01 g, 9.42 mmol) dissolved in dry dichloromethane (20 mL) was added dropwise to the solution at 0°C with stirring. The mixture was stirred for 1 h at 0°C and then for 16 h at room temperature. Then the solution was washed with 10% aqueous citric acid, saturated aqueous sodium chloride, 4% aqueous sodium hydrogen carbonate and saturated aqueous sodium chloride in this sequence. After residual water was removed using phase separation filter paper, the solvent was evaporated in vacuo to give a solid, which was subsequently purified on a column of silica gel with ethyl acetate/hexane 1:1. Recrystallization from methanol gave a white solid (2.77 g; 83.9%). M.p. 51.0–51.7°C; TLC: R_f=0.78 (ethyl acetate/hexane 1:1); ^{1}H NMR (400 MHz, $CDCl_3$, 25°C, TMS): δ = 0.88 (t, J=6.8 Hz, 6H, $(NCH_2CH_2(CH_2)_{13}CH_3)$, 1.24–1.29 (m, 52H, $NCH_2CH_2(CH_2)_{13}CH_3$), 1.46–1.60 (m, 6H, $NCH_2CH_2(CH_2)_{13}CH_3$, $BrCH_2CH_2CH_2CH_2CH_2CO$), 1.69 (m, 2H, $BrCH_2CH_2CH_2CH_2CH_2CO$), 1.88 (m, 2H, $BrCH_2CH_2CH_2CH_2CH_2CO$), 2.26 (t, J=7.3 Hz, 2H, $BrCH_2CH_2CH_2CH_2CH_2CO$), 3.15 (t, J=7.8 Hz, 2H, $NCH_2CH_2(CH_2)_{13}CH_3$), 3.30 (t, J=7.8 Hz, 2H, $NCH_2CH_2(CH_2)_{13}CH_3$), 3.41 (t, J=6.8 Hz, 2H, $BrCH_2CH_2$), 4.02 (d, J=5.9 Hz, 2H, $NHCH_2CO$), 6.63 ppm (br, 1H, $(CH_3)_3CONH$).

***N*,*N*-Dihexadecyl-*N*$^\alpha$-[6-(dimethylamino)hexanoyl]glycinamide (7)**: Dry dimethylamine gas was introduced into dry THF (100 mL) to saturate. To the dimethylamine saturated THF solution, **6** (1.40 g, 2.00 mmol) was added and the mixture was subsequently stirred at room temperature for 46 h. Then air was bubbled into the mixture in order to remove excess dimethylamine. The solvent was evaporated in vacuo and the residual solid was dissolved in chloroform (50 mL). The solution was then washed with saturated aqueous sodium chloride, 4% aqueous sodium hydrogen carbonate and saturated aqueous sodium chloride in this sequence. After removing residual water using phase separation filter paper, the solvent was evaporated in vacuo. The residue was purified by recrystallization from acetonitrile to give a white solid (1.14 g, 85.7%). M.p. 37.5–38.1°C; TLC: R_f=0.45 (chloroform/methanol 4:1); ^{1}H NMR (400 MHz, $CDCl_3$, 25°C, TMS): δ = 0.88 (t, J=6.8 Hz, 6H, $NCH_2CH_2(CH_2)_{13}CH_3$), 1.24–1.29 (m, 54H, $NCH_2CH_2(CH_2)_{13}CH_3$, $(CH_3)_2NCH_2CH_2CH_2CH_2$), 1.44–1.59 (m, 6H, $NCH_2CH_2(CH_2)_{13}CH_3$, $(CH_3)_2NCH_2CH_2CH_2CH_2CH_2CO$), 1.63–1.69 (m, 2H, $(CH_3)_2NCH_2CH_2CH_2CH_2CH_2CO$), 2.20 (s, 6H, $(CH_3)_2NCH_2CH_2$), 2.23–2.27 (m, 4H, $(CH_3)_2NCH_2CH_2CH_2CH_2CH_2CO$), 3.15 (t, J=7.8 Hz, 2H, $NCH_2CH_2(CH_2)_{13}CH_3$), 3.32 (t, J=7.8 Hz, 2H, $NCH_2CH_2(CH_2)_{13}CH_3$), 4.03 (d, J=5.9 Hz, 2H, $NHCH_2CO$), 6.64 ppm (br, 1H, $(CH_3)_3CONH$); elemental analysis calcd (%) for $C_{42}H_{85}N_3O_2$: C 75.95, H 12.90, N 6.33; found: C 75.67, H 12.80, N 6.30.

***N*,*N*-Dihexadecyl-*N*$^\alpha$-[6-[(3-triethoxysilyl)propyldimethylammonio]hexanoyl]glycinamide bromide (2)**: Compound **7** (0.300 g, 0.451 mmol) was added under a nitrogen atmosphere to a solution of 3-bromopropyltriethoxysilane (0.645 g, 3.61 mmol) in dry DMF (25 mL), and the mixture was stirred for 120 h. The solvent was evaporated in vacuo and the residue was purified by gel filtration chromatography (Sephadex LH-20, ethanol as the eluent) to afford a colorless viscous oil (0.417 g, 97.7%). TLC: R_f=0.49 (chloroform/ethanol 1:1); ^{1}H NMR (400 MHz, $CDCl_3$, 25°C, TMS): δ=0.66 (t, J=7.8 Hz, 2H, $SiCH_2$), 0.88 (t, J=6.6 Hz, 6H, $NCH_2CH_2(CH_2)_{13}CH_3$), 1.18–1.50 (m, 54H, $NCH_2CH_2(CH_2)_{13}CH_3$, $N^+CH_2CH_2CH_2CH_2CH_2CO$), 1.22 (t, J=7.0 Hz, 9H, CH_3CH_2OSi), 1.52–1.98 (m, 10H, $NCH_2CH_2(CH_2)_{13}CH_3$, $CH_2CH_2CH_2N^+CH_2CH_2CH_2CH_2CO$), 2.33 (t, J=7.0 Hz, 2H, $N^+CH_2CH_2CH_2CH_2CH_2CO$), 3.16 (t, J=7.8 Hz, 2H, $NCH_2CH_2(CH_2)_{13}CH_3$), 3.27–3.33 (m, 2H, $NCH_2CH_2(CH_2)_{13}CH_3$,), 3.34 (s, 6H, $CH_2N^+(CH_3)_2CH_2$), 3.46–3.56 (m, 4H, $CH_2CH_2N^+CH_2CH_2$), 3.83 (q, J=7.0 Hz, 6H, CH_3CH_2OSi), 4.01 (d, J=6.2 Hz, 2H, $NHCH_2CO$), 6.95 ppm (br, 1H,$CH_2CONHCH_2$); ^{13}C NMR (100 MHz, $CDCl_3$, 25°C, TMS): δ = 172.73, 167.62, 70.69, 65.87, 64.20, 58.77, 51.34, 47.13, 46.33, 41.06, 35.66,35.37, 31.98, 29.75, 29.42, 28.81, 27.71, 27.12, 26.98, 25.47, 24.67, 22.74, 22.28, 19.42, 18.36, 16.73, 14.15, 13.96, 6.91 ppm. HRMS (FAB$^+$): m/z: calcd for $C_{51}H_{106}N_3O_5Si$: 868.7901; found: 868.7606 $[M-Br]^+$; elemental analysis calcd (%) for $C_{51}H_{106}N_3BrO_5Si\cdot{}^1/_2H_2O$: C 63.91, H 11.25, N 4.38; found: C 63.98, H 11.29, N 4.40.

π–*A* Isotherm measurements: Surface pressure–molecular area (π–*A*) isotherms were measured using a computer controlled FSD-300 film balance system (USI System). Spectral grade benzene was used as the spreading solvent. The starting trough area was $150\times463\,mm^2$ and around 100 μL of the lipid solution was spread. Compression at a rate of $0.2\,mm\,s^{-1}$ started about 10 min after spreading. The subphase temperature was kept at $20.0\pm0.2\,°C$. The surface pressure was measured with a Wilhelmy plate, which had been calibrated using the transition pressure of an octadecanoic acid monolayer. The pH conditions of the subphase were controlled using H_2SO_4 and NH_4OH.

Preparation of the cerasomes: In the sol–gel process, a mutual solvent such as alcohol (for example, ethanol) is usually added to give a homogenized solution. In the present case, however, a mutual solvent should not be used as it would prevent disruption of the bilayer structure. Thus, the cerasomes were prepared using the following procedure, unless otherwise stated: 1–10 mg of **1** or **2** was suspended in 2–5 mL of H_2O under various pH conditions and dispersed by shaking with a vortex mixer until the oil droplets disappeared completely to give a translucent solution. The concentration of the lipid was controlled in a range of 1.0–5.0 $mmol\,dm^{-3}$. In some cases, the aqueous dispersion was ultrasonicated with a probe-type sonicator (Sonifier 250D, BRANSON).

^{1}H NMR spectroscopy: ^{1}H NMR spectra of the lipids dispersed in a deuterated solvent were measured by a JEOL JNM-LA400 NMR or JNM-EX270 spectrometer (400 and 270 MHz, respectively); sodium 3-(trimethylsilyl)propionate in D_2O was used as an internal reference. The pD value was adjusted by using aqueous deuterium chloride.

Mass spectrometry: For MS data of the cerasomes, free silanol and unhydrolyzed alkoxysilyl groups on the surface should be end-blocked by trimethylsilyl groups to avoid changes in the polymerization state during the measurements. Trimethylchlorosilane ($(CH_3)_3SiCl$) was employed for trimethylsilylation of the cerasome. Silanol and alkoxysilyl groups were capped with $(CH_3)_3SiOH$, generated by hydrolysis of $(CH_3)_3SiCl$. It is known that the original condensed form of silicates is maintained at 80–90% by this reaction.[44] All MS spectra were taken by using a Voyager DE-STR matrix-assisted laser desorption ionization time-of-flight (MALDI-TOF) mass spectrometer (PerSeptive Biosystems) operated at 25 kV accelerating voltage in linear mode with positive ionization. Dithranol was used as a matrix material.

Cryoscopic measurements: Cryoscopic determinations of the molecular weights of the cerasomes were carried out using trimethylsilylated samples in spectral grade benzene. The difference between the freezing point of the solution containing the trimethylsilylated sample and that of benzene itself, the freezing point depression, ΔT_f, was measured. The number-average molecular weight, M_n, was calculated from the following relationship, where g is the weight of the sample and G is the weight of benzene:

$$M_n = \frac{K_f \times 1000 \times g}{(G \times \Delta T_f)} \quad (1)$$

The constant, K_f, of the benzene was determined with benzophenone as a standard (the obtained value was 5.12). The cryoscopic measurements were carried out for a series of solutions at various concentrations in 1.0–5.0% (w/w). The number-average molecular weight of the sample was estimated by extrapolation from a plot of the relation between concentration and molecular weight.

Transmission electron microscopy (TEM): The aggregate structure of the cerasomes prepared from **1** and **2** were examined by TEM. In the case of cerasome **1**, the cerasome (0.5 mM) was prepared in aqueous HCl (pH 3) by vortex mixing and it was mixed with equal volume of 4 wt% of uranyl acetate and left for min. In the case of cerasome **2**, the cerasome (2.5 or 5 mM) was prepared directly in 2 wt% uranyl acetate solution by vortex mixing for 3 min. In some cases, the cerasome dispersions were ultrasonicated. An aliquot of these dispersions was cast on an ultrathin carbon-deposited Cu grid (Cu200, JEOL DATUM Ltd) and dried in a desiccator overnight followed by in vacuo for 1 h. TEM observations were carried out by using a JEOL JEM-3100FEF field emission electron microscope with an acceleration voltage of 300 kV. The images were obtained as zero-loss image through an in-column energy filter.

Surfactant dissolution of the cerasomes: The cerasomes were prepared by sonication of the dispersion sample using a probe-type sonicator for 20 min at 30 W and mixing in aqueous HCl (pH 3). For comparison conventional liposomes, derived from dimyristoylphosphatidylcholine (DMPC), were prepared using similar sonication conditions in pure water. The cerasomes and the DMPC liposomes obtained were characterized by light scattering intensity employing a fluorescence spectrophotometer (F-4500, HITACHI) for a 2 mL sample with a lipid concentration of 0.10 $mmol\,dm^{-3}$. The light scattering intensities were determined at a 90° angle. Aliquots of 50 mM Triton X-100 (TX-100) solution were added until the liposomes dissolved or 36 equivalents for the lipid.

Differential scanning calorimetry (DSC): The phase-transition temperature (T_m, temperature at a peak maximum of the DSC thermogram) of the cerasomes was measured with a differential scanning calorimeter (DSC-6100, Seiko Instruments). The aqueous dispersion (2 $mmol\,dm^{-3}$) was weighed and sealed in a silver capsule. The enthalpy change for the phase transition (ΔH) was determined by measuring the peak area of the DSC thermogram.

Zeta-potential measurements: Zeta-potentials of the cerasomes were evaluated by using an instrument for electrophoretic light scattering with a laser Doppler system (ELS-6000, Otsuka Electronics). For the zeta-potential measurements, the cerasome was prepared in aqueous NaCl (10 $mmol\,dm^{-3}$) upon sonication of the dispersion sample with a probe-type sonicator for 20 min at 30 W. The pH of the solution was adjusted by addition of HCl or NaOH.

Dynamic light scattering (DLS): The hydrodynamic diameter and its polydispersity index of the cerasomes were measured by a dynamic light scattering spectrophotometer (DLS-6000HL, Otsuka Electronics). The instrument consisted of a He/Ne laser, which was operated at 633 nm and 10 mW. The data obtained was analyzed using the cumulant method.

Acknowledgements

This work was supported by the Japan Society for the Promotion of Science, Grant-in-Aid for Scientific Research. The authors deeply thank Mr. K. Furusho, Graduate School of Materials Science, NAIST, for TEM measurements.

[1] a) C. Sanchez, F. Ribot, *New J. Chem.* **1994**, *18*, 1007; b) C. Sanchez, G. J. de A. A. Soler-Illia, F. Ribot, T. Lalot, C. R. Mayer, V. Cabuil, *Chem. Mater.* **2001**, *13*, 3061.
[2] a) *Organic/Inorganic Hybrid Materials, Vol. 519* (Eds.: R. M. Laine, C. Sanchez, C. J. Brinker, E. Giannelis), *Mater. Res. Soc. Symp. Proc.*, Materials Research Society, Warrendale, PA, **1998**; b) *Organic/Inorganic Hybrid Materials II, Vol. 576* (Eds.: L. Klein, M. DeGuire, F. Lorraine, J. Mark), *Mater. Res. Soc. Symp. Proc.*, Materials Research Society, Warrendale, PA, **1999**.
[3] a) H. Schmidt, *J. Sol-Gel Sci. Technol.* **1994**, *1*, 217; b) J. D. Mackenzie, *J. Sol-Gel Sci. Technol.* **1994**, *2*, 81.
[4] G. Schottner, *Chem. Mater.* **2001**, *13*, 3422.
[5] a) C. J. Brinker, G. W. Scherer, *Sol-Gel Science, The Physics and Chemistry of Sol-Gel Processing*, Academic Press, San Diego, CA, **1990**; b) *Sol-Gel Science and Technology* (Eds.: E. J. A. Pope, S. Sakka, L. C. Klein), American Ceramic Society, Westerville, OH, **1995**; c) A. C. Pierre, *Introduction to Sol-Gel Processing*, Kluwer Academic, Boston, MA, **1998**.
[6] a) S. Mann, *Angew. Chem.* **2000**, *112*, 3532; *Angew. Chem. Int. Ed.* **2000**, *39*, 3392; b) H. Cölfen, S. Mann, *Angew. Chem.* **2003**, *115*, 2452; *Angew. Chem. Int. Ed.* **2003**, *42*, 2350.
[7] J. H. Rouse, B. A. MacNeill, G. S. Ferguson, *Chem. Mater.* **2000**, *12*, 2502.
[8] A. Ulman, *Chem. Rev.* **1996**, *96*, 1533.

[9] a) G. A. Ozin, *Chem. Commun.* **2000**, 419; b) S. Oliver, A. Kuperman, G. A. Ozin. *Angew. Chem.* **1998**, *110*, 48; *Angew. Chem. Int. Ed.* **1998**, *37*, 46.
[10] D. M. Dabbs, I. A. Aksay, *Annu. Rev. Phys. Chem.* **2000**, *51*, 601.
[11] B. J. Scott, G. Wirnsberger, G. D. Stucky, *Chem. Mater.* **2001**, *13*, 3140.
[12] K. J. C. van Bommel, A. Friggeri, S. Shinkai, *Angew. Chem.* **2003**, *115*, 1010; *Angew. Chem. Int. Ed.* **2003**, *42*, 980.
[13] a) T. Yanagisawa, T. Shimizu, K. Kuroda, C. Kato, *Bull. Chem. Soc. Jpn.* **1990**, *63*, 988; b) M. Ogawa, K. Kuroda, *Bull. Chem. Soc. Jpn.* **1997**, *70*, 2593; c) M. Ogawa, *J. Am. Chem. Soc.* **1994**, *116*, 7941.
[14] a) S. Inagaki, S. Guan, Y. Fukushima, T. Ohsuna, O. Terasaki, *J. Am. Chem. Soc.* **1999**, *121*, 9611; b) S. Guan, S. Inagaki, T. Ohsuna, O. Terasaki, *J. Am. Chem. Soc.* **2000**, *122*, 5660; c) S. Inagaki, S. Guan, T. Ohsuna, O. Teraski, *Nature* **2002**, *416*, 304.
[15] a) C. T. Kresge, M. E. Leonowicz, W. J. Roth, J. C. Vartuli, J. S. Beck, *Nature* **1992**, *359*, 710; b) J. S. Beck, J. C. Vartuli, W. J. Roth, M. E. Leonowitz, C. T. Kresge, K. D. Schmitt, C. T.-W. Chu, D. H. Olson, E. W. Sheppard, S. B. McCullen, J. B. Higgins, J. L. Schlenker, *J. Am. Chem. Soc.* **1992**, *114*, 10834.
[16] M. Kruk, V. Antochshuk, M. Jaroniec, *J. Phys. Chem. B* **2000**, *104*, 11465.
[17] a) M. Antonietti, *Langmuir* **1998**, *14*, 2027; b) C. G. Göltner, S. Henke, M. C. Weissenberger, M. Antonietti, *Angew. Chem.* **1998**, *110*, 633; *Angew. Chem. Int. Ed.* **1998**, *37*, 613; c) C. G. Göltner, B. Berton, E. Krämer, M. Antonietti, *Adv. Mater.* **1999**, *11*, 395.
[18] N. A. Melosh, P. Lipic, F. S. Bates, F. Wudl, G. D. Stucky, G. H. Fredrickson, B. F. Chmelka, *Macromolecules* **1999**, *32*, 4332.
[19] a) P. Schmidt-Winkel, C. J. Glinka, G. D. Stucky, *Langmuir* **2000**, *16*, 356; b) P. Feng, X. Bu, G. D. Stucky, D. J. Pine, *J. Am. Chem. Soc.* **2000**, *122*, 994.
[20] S. D. Sims, D. Walsh, S. Mann, *Adv. Mater.* **1998**, *10*, 154.
[21] a) Y. Ono, K. Nakashima, M. Sano, Y. Kanekiyo, K. Inoue, J. Hojo, S. Shinkai, *Chem. Commun.* **1998**, 1477; b) J. H. Jung, H. Kobayashi, M. Masuda, T. Shimizu, S. Shinkai, *J. Am. Chem. Soc.* **2001**, *123*, 8785; c) J. H. Jung, S. Shinkai, T. Shimizu, *Chem. Rec.* **2003**, *3*, 212; d) T. Hatano, A.-H. Bae, M. Takeuchi, N. Fujita, K. Kaneko, H. Ihara, M. Takafuji, S. Shinkai, *Angew. Chem.* **2004**, *116*, 471; *Angew. Chem. Int. Ed.* **2004**, *43*, 465.
[22] K. Sakata, T. Kunitake, *J. Chem. Soc. Chem. Commun.* **1990**, 504.
[23] a) D. H. W. Hubert, M. Jung, P. M. Frederik, P. H. H. Bomans, J. Meuldijkm A. L. German, *Adv. Mater.* **2000**, *12*, 1286; b) D. H. W. Hubert, M. Jung, A. L. German, *Adv. Mater.* **2000**, *12*, 1291.
[24] Q. Huo, D. I. Margolese, G. D. Stucky, *Chem. Mater.* **1996**, *8*, 1147.
[25] a) A. Shimojima, Y. Sugahara, K. Kuroda, *Bull. Chem. Soc. Jpn.* **1997**, *70*, 2847; b) A. Shimojima, Y. Sugahara, K. Kuroda, *J. Am. Chem. Soc.* **1998**, *120*, 4528; c) D. Mochizuki, A. Shimojima, K. Kuroda, *J. Am. Chem. Soc.* **2002**, *124*, 12082; d) A. Shimojima, K. Kuroda, *Angew. Chem.* **2003**, *115*, 4191; *Angew. Chem. Int. Ed.* **2003**, *42*, 4057.
[26] a) J. J. E. Moreau, L. Vellutini, M. Wong Chi Man, C. Bied, J. L. Bantignies, P. Dieudonné, J. L. Sauvajol, *J. Am. Chem. Soc.* **2001**, *123*, 7957; b) O. J. Dautel, J.-P. Lélе-Porte, J. J. E. Moreau, M. Wong Chi Man, *Chem. Commun.* **2003**, 2662; c) J. J. E. Moreau, B. P. Pichon, M. Wong Chi Man, C. Bied, H. Pritzkow, J.-L. Bantignies, P. Dieudonné, J.-L. Sauvajol, *Angew. Chem.* **2004**, *116*, 205; *Angew. Chem. Int. Ed.* **2004**, *43*, 203.
[27] a) E. Ruiz-Hitzky, S. Letaïef, V. Prévot, *Adv. Mater.* **2002**, *14*, 439; b) E. Ruiz-Hitzky, *Chem. Rec.* **2003**, *3*, 88.
[28] a) Q. Zhang, K. Ariga, A. Okabe, T. Aida, *J. Am. Chem. Soc.* **2004**, *126*, 988; b) K. Ariga, *Chem. Rec.* **2004**, *3*, 297.
[29] a) K. Katagiri, K. Ariga, J. Kikuchi, *Chem. Lett.* **1999**, 661; b) K. Ariga, K. Katagiri, J. Kikuchi, *Kobunshi Ronbunshu* **2000**, *57*, 251; c) K. Katagiri, K. Ariga, J. Kikuchi, *Stud. Surf. Sci. Catal.* **2001**, *132*, 599; d) K. Katagiri, R. Hamasaki, K. Ariga, J. Kikuchi, *J. Am. Chem. Soc.* **2002**, *124*, 7892; e) K. Katagiri, R. Hamasaki, K. Ariga, J. Kikuchi, *Langmuir* **2002**, *18*, 6709; f) K. Katagiri, R. Hamasaki, K. Ariga, J. Kikuchi, *J. Sol-Gel Sci. Technol.* **2003**, *26*, 393.
[30] A. D. Bangham, R. W. Horne, *J. Mol. Biol.* **1964**, *8*, 660.
[31] G. Sessa, G. Weissmann, *J. Biol. Chem.* **1968**, *243*, 4364.
[32] a) T. Kunitake, Y. Okahata, *J. Am. Chem. Soc.* **1977**, *99*, 3860; b) T. Kunitake, in *Comprehensive Supramolecular Chemistry, Vol. 9* (Eds.: J. L. Atwood, J. E. D. Davies, D. D. MacNicol, F. Vögtle, J.-M. Lehn), Pergamon, Oxford (UK), **1996**, p. 351.
[33] H. Ringsdolf, B. Schlarb, J. Venzmer, *Angew. Chem.* **1988**, *100*, 117; *Angew. Chem. Int. Ed. Engl.* **1988**, *27*, 113.
[34] Y. Murakami, J. Kikuchi, in *Bioorganic Chemistry Frontiers, Vol. 2* (Ed.: H. Duga), Springer, Berlin, **1991**, p. 73.
[35] a) S. L. Regen, A. Singh, G. Oehme, M. Singh, *J. Am. Chem. Soc.* **1982**, *104*, 791; b) R. L. Juliano, S. L. Regen, M. Singh, M. J. Hsu, A. Singh, *Bio/Technology* **1983**, *1*, 882; c) S. K. M. Davidson, S. L. Regen, *Chem. Rev.* **1997**, *97*, 1269.
[36] a) J. N. Israelachivili, D. J. Mitchell, B. W. Ninham, *J. Chem. Soc. Faraday Trans. 2* **1976**, *72*, 1525; b) D. J. Mitchell, B. W. Ninham, *J. Chem. Soc. Faraday Trans. 2* **1981**, *77*, 601;
[37] H. Brockerhoff, in *Bioorganic Chemistry, Vol. 3* (Ed.: E. E. Tamelen), Academic Press, New York, **1977**, Chapter 1.
[38] Z. Zhang, Y. Tanigami, R. Terai, H. Wakabayashi, S. Sakka, *J. Phys. Chem. B* **1997**, *101*, 1328.
[39] a) T. M. Sisson, H. G. Lamparski, S. Kölchens, A. Elayadi, D. F. O'Brien, *Macromolecules* **1996**, *29*, 8321; b) D. F. O'Brien, B. Armitage, A. Benedicto, D. E. Bennett, H. G. Lamparski, Y.-S. Lee, W. Srisiri, T. M. Sisson, *Acc. Chem. Res.* **1998**, *31*, 861; c) S. Liu, D. F. O'Brien, *Macromolecules* **1999**, *32*, 5519; d) S. Liu, D. F. O'Brien, *J. Am. Chem. Soc.* **2002**, *124*, 6037; e) A. Mueller, D. F. O'Brien, *Chem. Rev.* **2002**, *102*, 727.
[40] Y. Sasaki, M. Yamada, T. Terashima, J.-F. Wang, M. Hashizume, S.-D. Fan, J. Kikuchi, *Kobunshi Ronbunshu* **2004**, *61*, 541.
[41] R. K. Iler, *The Chemistry of Silica*, Wiley, New York, **1979**.
[42] H. Nishimori, M. Tatsumisago, T. Minami, *Bull. Chem. Soc. Jpn.* **1996**, *69*, 815.
[43] K. Ariga, Y. Okahata, *J. Am. Chem. Soc.* **1989**, *111*, 5618.
[44] a) C. W. Lentz, *Inorg. Chem.* **1964**, *3*, 574; b) L. S. D. Glasser, S. K. Sharma, *Br. Polym. J.* **1974**, *6*, 283; c) B. R. Currel, J. R. Parsonage, *J. Macromol. Chem.* **1981**, *A16*, 141.

Received: February 1, 2007
Published online: April 3, 2007

